

Age and metallicity estimates from high-resolution galaxy spectra: application to early-type galaxies

Anna Gallazzi¹, S. Charlot^{1,2}, S. D. M. White¹
and J. Brinchmann^{3,1}

¹Max-Planck-Institut für Astrophysik, Garching bei München, Germany email:
gallazzi@mpa-garching.mpg.de

²Institut d'Astrophysique du CNRS, Paris, France

³Centro de Astrofísica da Universidade do Porto, Porto, Portugal

Abstract. We present a method for deriving light-weighted stellar metallicities and ages from high-resolution galaxy spectra, based on the new population synthesis code of Bruzual & Charlot (2003). The method relies on the simultaneous fit of several optical spectral absorption features that are sensitive to either age or metallicity, but not to the α -elements abundance ratio. We have constructed a library of stochastic star formation histories, which we have used to derive median-likelihood estimates of ages and metallicities for $\sim 10^5$ galaxies extracted from the Sloan Digital Sky Survey Data Release One (SDSS DR1), spanning the full range in star formation activities, from dormant early type to actively star forming. Here we discuss the results for early-type galaxies. We show that the $g-r$, M_r color-magnitude relation for these galaxies is driven primarily by changes in metallicity and in heavy-element abundance ratios. Changes in light-weighted age contribute mainly to the scatter about the relation. This is consistent with previous interpretations of this relation based on lower resolution models.

1. Introduction

The ages and metallicities of the stellar populations in galaxies are direct signatures of the physical processes that were important in their formation and evolution. If we can interpret the light emitted by galaxies in terms of stellar ages and metallicities, we will therefore be able to better constrain the evolution of galaxies and how it depends on environment. In practice, interpretations of galaxy spectra using population synthesis models have been impaired by the fact that age, metallicity and attenuation by dust all have a similar influence on the integrated colors and low-resolution spectra of galaxies (e.g., Worthey 1994). The expectation is that this degeneracy can be broken by appealing to refined spectral diagnostics involving individual stellar absorption-line features (e.g., Vazdekis 1999).

We present here a method for estimating light-weighted stellar metallicities and ages from high-resolution galaxy spectra, based on the new population synthesis code of Bruzual & Charlot (2003) (hereafter BC03). The method consists in comparing the observed strengths of selected optical absorption features with the predictions of models drawn from a comprehensive library of star formation histories. An important requirement of this method is that the spectral absorption features be measured in the same way in the observations and in the model spectra. The method can be applied to all types of galaxies, from early type to actively star forming. We have used this approach to derive light-weighted stellar metallicities and ages for $\sim 10^5$ galaxies extracted from the SDSS-DR1. We present here the results for a subsample of 5343 high signal-to-noise

ratio, early-type galaxies in the narrow redshift range $0.02 < z < 0.08$. We focus in particular on the interpretation of one of the main observational relations for elliptical: the color-magnitude relation.

2. High-resolution spectra

2.1. Models

To examine the way in which physical parameters such as stellar age and metallicity can be extracted from high-resolution galaxy spectra, we use the recent population synthesis models of Bruzual & Charlot (2003). The models have a resolution of 3 \AA across the whole wavelength range from 3200 \AA to 9500 \AA for a wide range of metallicities. These predictions are based on a newly available library of observed stellar spectra (Le Borgne et al. 2003).

2.2. Observations

We analyze a sample of nearly 10^5 galaxies drawn from the SDSS-DR1. The spectra are obtained with a $3''$ diameter fiber, positioned as close as possible to the center of the target galaxy. The wavelength coverage is from 3800 \AA to 9200 \AA with a resolving power $\lambda/\Delta\lambda \sim 1800$. The spectroscopic sample is complete to a petrosian r -band magnitude limit $r < 17.77$. To measure stellar absorption features in galaxies with nebular emission, it is important to first remove emission lines. This is performed using the procedure outlined by Tremonti et al. 2004, which fits the emission-line-free region of the spectrum with a set of template spectra (see also Kauffmann et al. 2003 and Brinchmann et al. 2003 for more details).

2.3. Stellar absorption-line indices

Previous studies have made extensive use of the Lick-IDS system of absorption line indices. This system includes 25 spectral features across the wavelength range from 4000 \AA to 6400 \AA . These are traditionally parametrized as a function of stellar parameters and observed spectra have had to be degraded to match the instrumental response of the Lick-IDS spectrograph (Burstein et al. 1984, Gorgas et al. 1993, Worthey et al. 1994, Trager et al. 1998). Here we improve on these studies by measuring the indices directly on the model and galaxy spectra using the bandpass definitions from Worthey & Ottaviani (1997), hence circumventing the need to degrade the spectra. As described in Bruzual & Charlot (2003), some of these spectral features are not well reproduced by the models. This is likely due to a discrepancy in element abundance ratios between SDSS galaxies and the models, that rely on the spectra of stars with scaled-solar abundances. The influence of variations in abundance ratios on index strengths has been investigated in several studies (Tripicco & Bell 1995, Tantalo et al. 1998, Trager et al. 2000, Vazdekis et al. 2001, Thomas et al. 2003). Due to the approximately constant (solar) abundance ratios of BC03 models, the spectral indices that can be used to constrain the fit are those that do not show any dependence on element abundance ratio. With this purpose, three ‘composite’ indices that are sensitive to metallicity but not to α/Fe have been measured: the new $[\text{MgFe}]'$ proposed by Thomas et al. (2003), $[\text{Mg}_1\text{Fe}]$ and $[\text{Mg}_2\text{Fe}]$ as defined in Bruzual & Charlot (2003).

3. Age and metallicity estimates

We adopt a Bayesian statistical approach to derive estimates of stellar metallicity and light-weighted age for the galaxies of our sample. The goal of the Bayesian statistics is to

obtain the likelihood distribution of a given parameter X in the space of all possible values of X . This is obtained by comparing the observational data with a set of models that populate the space of all possible X according to a prior distribution, that represents our knowledge about the relative likelihood of the various X values in absence of any data. We generate a library of 150,000 Monte Carlo realizations of a full range of physically plausible star formation histories (SFHs). These are composed of an underlying continuous SFH with superposed random bursts of star formation (following Kauffmann *et al.* 2003). The models are distributed uniformly in the space of the parameters that define the models; in particular, they are distributed logarithmically in metallicity from 0.02 to 2.5 solar. All stars in a given model have a fixed metallicity, which we interpret as the light-weighted metallicity.

The probability distribution function (PDF) for a given parameter allows us to derive an estimate of the parameter (the mode or median of the distribution) as well as the error associated with this estimate (the range between the 16th and the 84th percentiles). Each model in the library is assigned a likelihood, $P = \exp(-\chi^2/2)$, where χ^2 is calculated by comparing the strength of a set of spectral features measured from the observed spectra with that measured from the model, normalising by the measurement error on the indices. Since the measure of some absorption indices depends also on the galaxy velocity dispersion, only models with velocity dispersion within 15 km/s of the observed one are considered. The absorption indices that can be chosen to constrain the fit have to be well reproduced by BC03 models and they have to be independent of α/Fe ratio (according to Worthey *et al.* 1994 and Thomas *et al.* 2003), since the models do not have a variable element abundance ratio. Our preferred choice of indices is the set composed of the 4000Å-break, the Balmer lines $H\beta$, $H\delta+H\gamma$, and the three composite indices $[\text{MgFe}]'$, $[\text{Mg}_1\text{Fe}]$, $[\text{Mg}_2\text{Fe}]$.

In Fig. 1 we show the PDF of stellar metallicity (left) and r -band weighted age (right) of four galaxies chosen in different positions along the $H\delta - D_n(4000)$ plane (as indicated in the top panels). The results obtained using only $D_n(4000)$ and Balmer lines to constrain the fit are shown in the bottom panels: while ages are already well constrained, including more metallicity-sensitive indices (upper panels) is required to have good estimates of metallicity. In this plot galaxies are ordered from left to right with increasing value of 4000Å-break: this seems to correspond to a sequence also in metallicity and age. Apart from the choice of indices, the quality of the data also determines the results and their accuracy. We have checked that a median S/N ratio per pixel of at least 20 is required to obtain reasonable estimates of metallicity.

4. The color-magnitude relation of early-type galaxies

Our estimates of metallicity and age allow us to explore some of the well-known observational relations between the physical parameters of galaxies. In this work we focus our attention on the relation between color and absolute magnitude for early-type galaxies. We define our sample of early-type galaxies by taking a concentration parameter $R_{90}/R_{50} > 2.6$ (Strateva *et al.* 2001) and $D_n(4000) > 1.8$, in the redshift range between 0.02 and 0.08. Here we present results for only 5343 galaxies with $S/N > 20$. The color-magnitude relation has often been interpreted as a relation between metallicity and mass, by looking at the correlation of spectral features such as Mg_2 or CN with luminosity and color (e.g., Faber 1973, Worthey *et al.* 1994). Fig. 2 shows the (k-corrected) $g - r, M_r$ color-magnitude relation for our sample. In Fig. 2a the relation has been binned and coded reflecting the average stellar metallicity (derived from our analysis) of the galaxies falling into each bin. The same has been done in Fig. 2b to reflect the average α/Fe

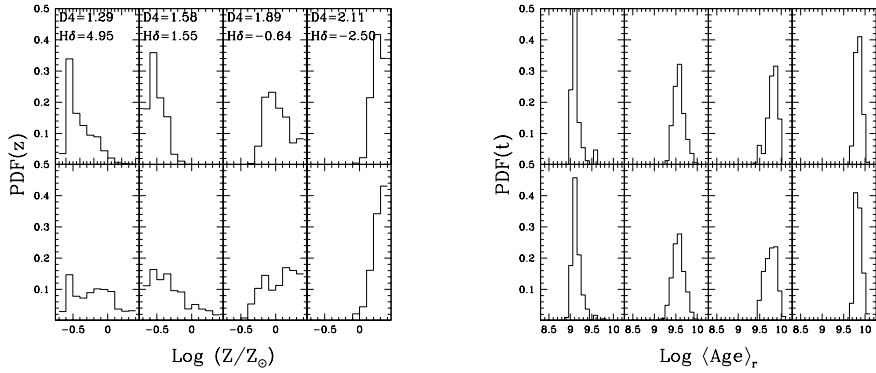


Figure 1. Probability distribution functions of stellar metallicity (left) and r -band weighted age (right) of four galaxies of our sample in different positions along the $H\delta$ - $D_n(4000)$ relation (the values of the two indices are indicated in the top panels). Results obtained using only $D_n(4000)$ and Balmer lines are shown in the bottom panels, while those obtained by adding Mg+Fe composite indices in the upper panels.

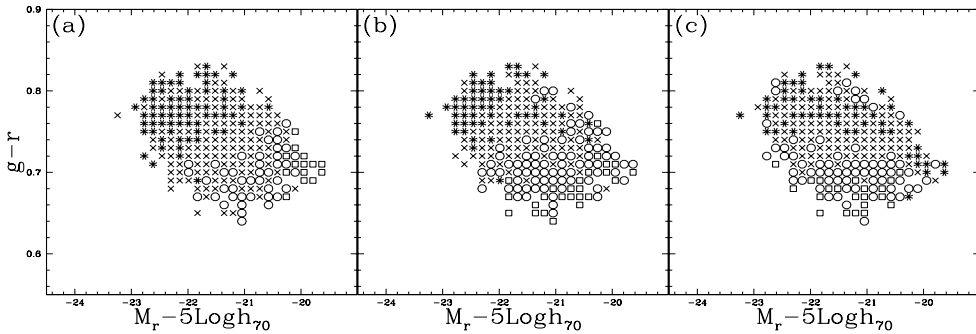


Figure 2. The $g-r$, M_r color-magnitude relation is shown for our sample of early-type galaxies ($R_{90}/R_{50} > 2.6$ and $D_n(4000) > 1.8$) as a function of stellar metallicity (a), $Mg_2/\langle Fe \rangle$ (b) and r -band weighted age (c). The different symbols indicate different average values of the parameter in each bin of absolute magnitude and $g-r$ color. Squares represent $\text{Log}(Z/Z_\odot) \leq 0.06$, $Mg_2/\langle Fe \rangle \leq 0.08$ and $\text{Log}\langle \text{Age} \rangle_r \leq 9.75$. Circles represent $0.06 < \text{Log}(Z/Z_\odot) \leq 0.15$, $0.08 < Mg_2/\langle Fe \rangle \leq 0.09$, $9.75 < \text{Log}\langle \text{Age} \rangle_r \leq 9.8$. Crosses represent $0.15 < \text{Log}(Z/Z_\odot) \leq 0.21$, $0.09 < Mg_2/\langle Fe \rangle \leq 0.1$, $9.8 < \text{Log}\langle \text{Age} \rangle_r \leq 9.83$. Stars represent $\text{Log}(Z/Z_\odot) > 0.21$, $Mg_2/\langle Fe \rangle > 0.1$, $\text{Log}\langle \text{Age} \rangle_r > 9.83$.

ratio, as indicated by the $Mg_2/\langle Fe \rangle$ index (where $\langle Fe \rangle$ is the average of Fe5270 and Fe5335 index strengths), and in Fig. 2c to reflect the r -band light-weighted age. There is a marked gradient in metallicity along the relation, with fainter galaxies being more metal-poor than brighter galaxies. In addition the $Mg_2/\langle Fe \rangle$ index ratio also increases with increasing luminosity and color. It appears that, therefore, although stellar metallicity is responsible in generating the observational relation between color and luminosity, element abundance ratio is another important controlling parameter. On the other hand, the light-weighted age of these early-type galaxies varies over a narrow range of about 2 Gyr, with a gradient almost parallel to the color axis. This difference in light-weighted age contributes to the scatter about the observed relation.

Acknowledgements

AG and SC thank the Alexander von Humboldt Foundation, the Federal Ministry of Education and Research and the Programme for Investment in the Future (ZIP) of the German Government for financial support.

JB acknowledges the support of an ESA post-doctoral fellowship. Funding for the creation and distribution of the SDSS Archive has been provided by the Alfred P. Sloan Foundation, the Participating Institutions, the National Aeronautics and Space Administration, the National Science Foundation, the U.S. Department of Energy, the Japanese Monbukagakusho, and the Max Planck Society. The SDSS Web site is <http://www.sdss.org/>.

References

- Brinchmann, J., Charlot, S., White, S. D. M., Tremonti, C., Kauffmann, G., Heckman, T. & Brinkmann, J. 2003 *astro-ph/0311060*
- Bruzual, G., & Charlot, S. 2003 *MNRAS* **344**, 1000–1028
- Burstein, D., Faber, S. M., Gaskell, C. M., & Krumm, N. 1984 *ApJ* **287**, 586–609
- Faber, S. M. 1973 *ApJ* **179**, 731–754
- Gorgas, J., Faber, S. M., Burstein, D., Gonzalez, J. J., Courteau, S., & Prosser, C. 1993 *ApJS* **86**, 153–198
- Kauffmann, G. et al. 2003 *MNRAS* **341**, 33–53
- Le Borgne, J.-F. et al. 2003 *A&A* **402**, 433–442
- Schlegel, D. J., Finkbeiner, D. P., & Davis, M. 1998 *ApJ* **500**, 525–553
- Strateva, I. et al. 2001 *AJ* **122**, 1861–1874
- Tantalo, R., Chiosi, C., & Bressan, A. 1998 *A&A* **333**, 419–432
- Thomas, D., Maraston, C., & Bender, R. 2003 *MNRAS* **339**, 897–911
- Trager, S. C., Worthey, G., Faber, S. M., Burstein, D., & Gonzalez, J. J. 1998 *ApJS* **116**, 1–28
- Trager, S. C., Faber, S. M., Worthey, G., & González, J. J. 2000 *AJ* **119**, 1645–1676
- Tremonti, C. A., Heckman, T. M., Kauffmann, G., Charlot, S., Brinchmann, J. 2004 *submitted to ApJ*
- Tripicco, M. J. & Bell, R. A. 1995 *AJ* **110**, 3035–3049
- Vazdekis, A. 1999 *ApJ* **513**, 224–241
- Vazdekis, A., Salaris, M., Arimoto, N., & Rose, J. A. 2001 *ApJ* **549**, 274–280
- Worthey, G., Faber, S. M., Gonzalez, J. J., & Burstein, D. 1994 *ApJS* **94**, 687–722
- Worthey, G. 1994 *ApJS* **95**, 107–149
- Worthey, G. & Ottaviani, D. L. 1997 *ApJS* **111**, 377–386